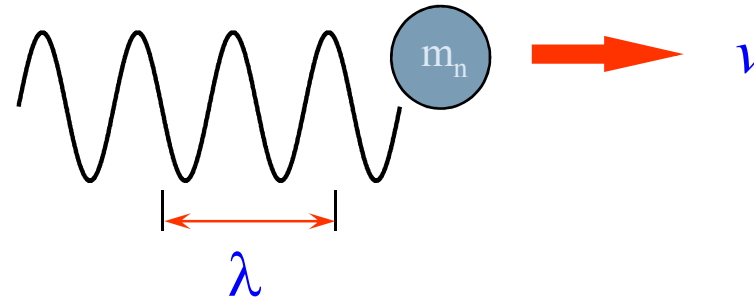


Quasi-elastic scattering

Theory and experiment hand in hand

Julia S Higgins
Imperial College London

The Neutron



Wave-particle duality

$$\lambda = \frac{h}{m_n \nu}$$

de Broglie
(1924)

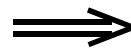
$$m_n = 1.674 \times 10^{-27} \text{ kg}$$

Thus:

$$\lambda \sim 10^{-10} \text{ m}$$

$$E \sim k_B T$$

+ Neutrons scattered by nucleus



isotopic substitution - labelling

$$b_H = -3.74 \times 10^{-15} \text{ m}$$

$$b_D = +6.67 \times 10^{-15} \text{ m}$$

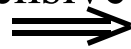
+ Neutrons highly penetrating & non-destructive



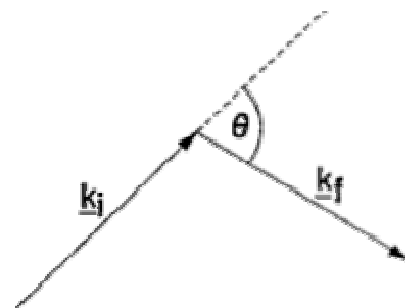
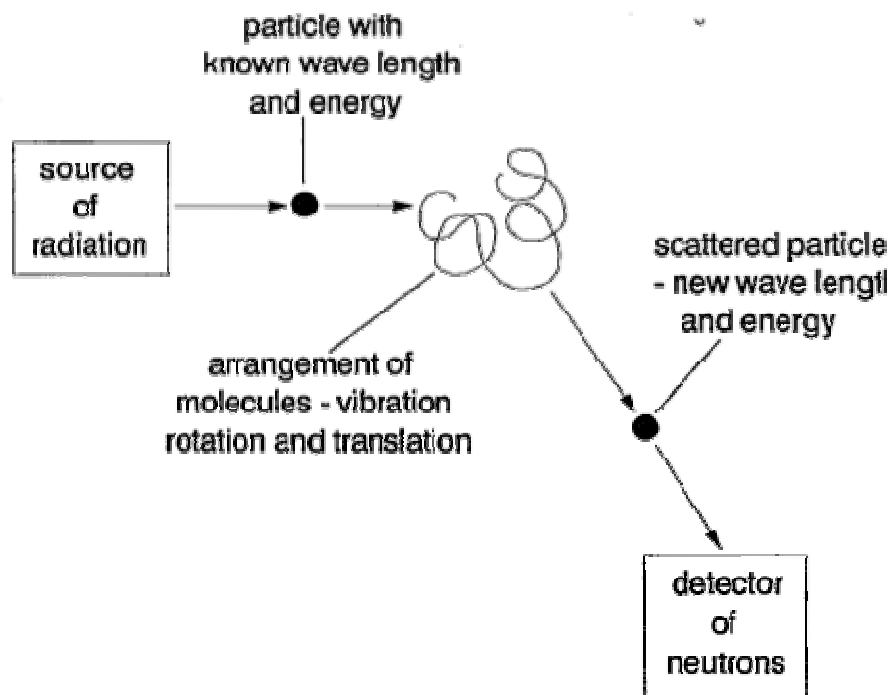
complex sample environment

repetitive measurements

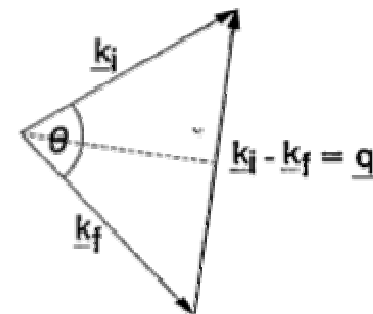
- Very Expensive



nuclear reactors or spallation sources

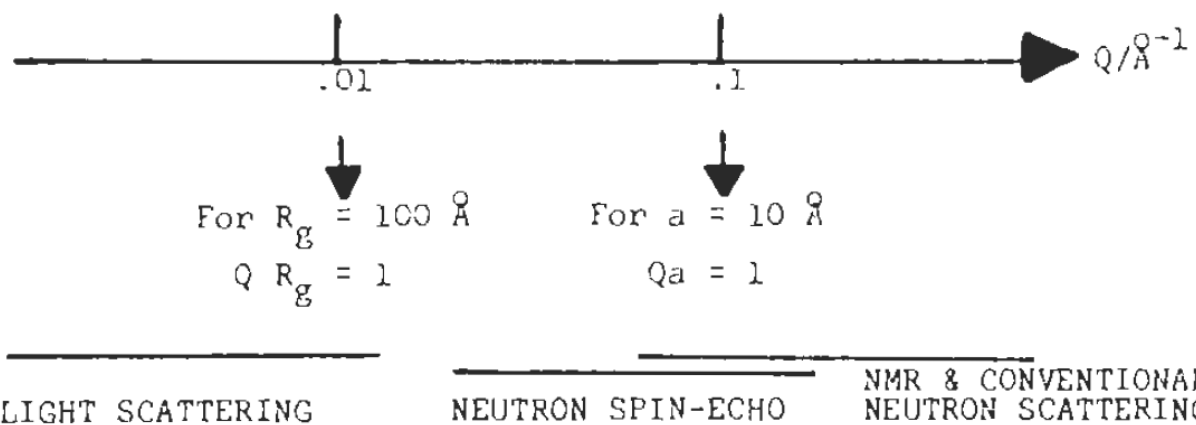
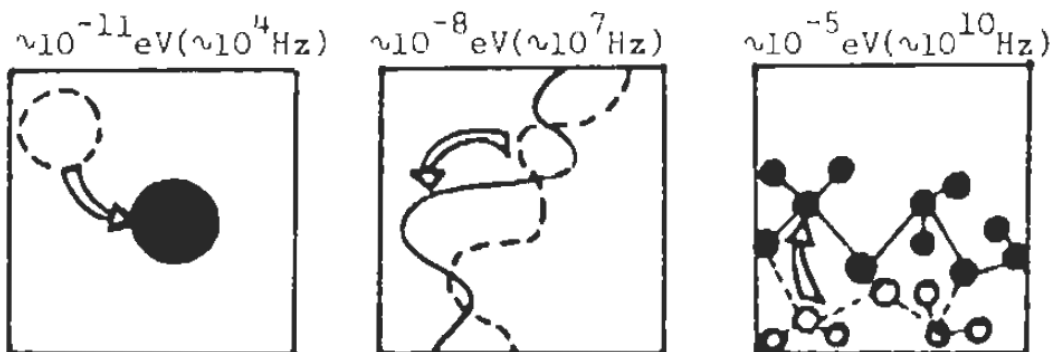


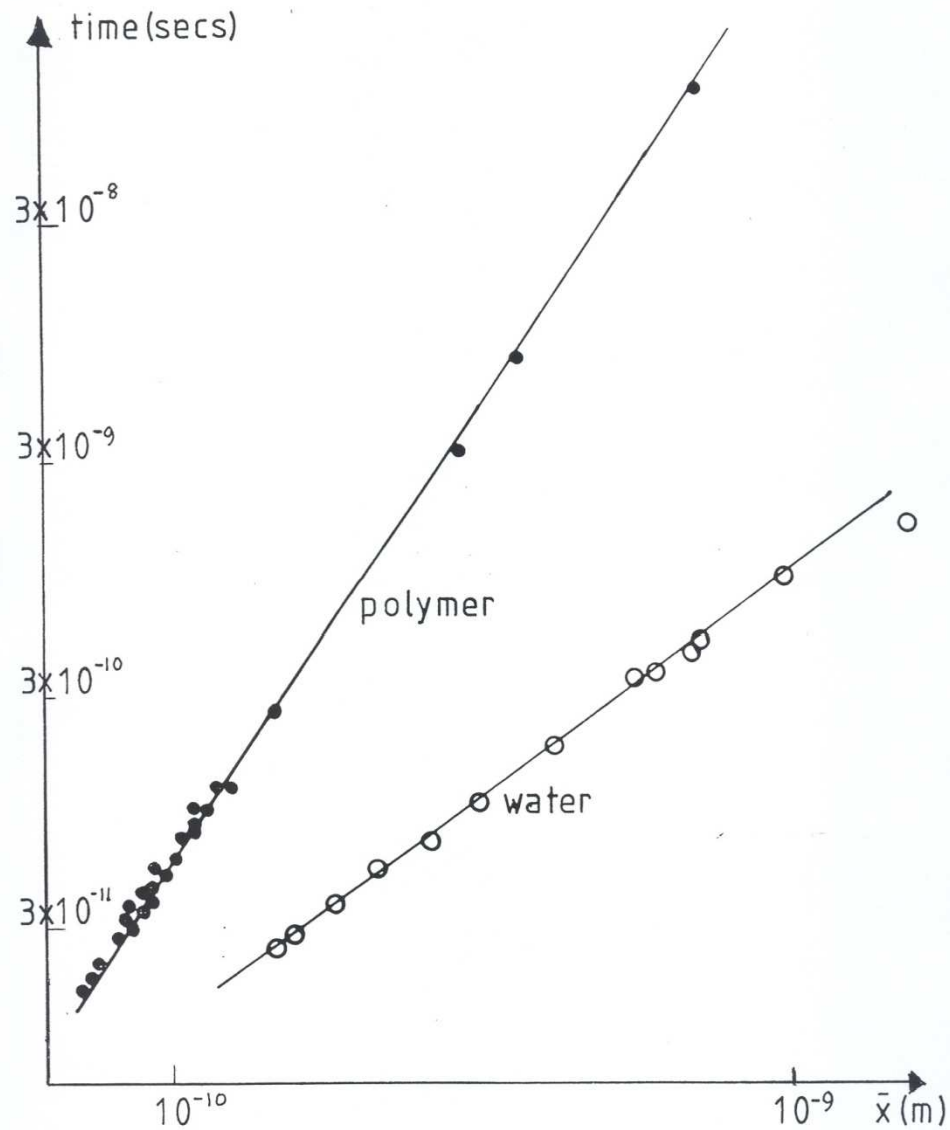
$$\left. \begin{aligned} k_i &= k_f = 2\pi/\lambda \\ q &= 2k_i \sin \theta/2 \\ &= 2k_f \sin \theta/2 \end{aligned} \right\} = (4\pi/\lambda) \sin \theta/2$$



$$\begin{aligned} k_i &= |\underline{k}_i| \\ k_f &= |\underline{k}_f| \\ q &= |\underline{q}| \end{aligned}$$

TYPICAL ENERGIES OF MOTION (& CORRESPONDING FREQUENCIES)





How far does a molecule move in a unit of time?

QUASI-ELASTIC SCATTERING OF NEUTRONS BY DILUTE POLYMER SOLUTIONS: I. FREE-DRAINING LIMIT

P.-G. de GENNES

*Laboratoire de Physique des Solides associé au C.N.R.S.
Faculté des Sciences d'ORSAY - 91 - France*

(Received 20 June 1966)

Abstract

In the so-called "free-draining limit", successive units of a long molecule equalise their average orientation by a diffusion process along the chain. For low values of the momentum transfer $\hbar\mathbf{q}$ and of the energy transfer $\hbar\omega$ the dynamical form factor $S(\mathbf{q}, \omega)$ for neutron scattering is controlled by this effect, and is independent of the vibrational spectrum. In this regime, we show that the frequency width $\Delta\omega_{\mathbf{q}}$ of $S(\mathbf{q}, \omega)$ is small and proportional to q^4 . The unusual q^4 law is related to the fact that, in a time t , a signal travels a distance $d \sim \sqrt{t}$ along the chain, but the corresponding distance in space is only of order $d^{1/2}$ for a coiled polymer. On the other hand, if the chain is stretched this argument breaks down and the width $\Delta\omega_{\mathbf{q}}$ for coherent scattering is predicted to increase.

QUASI-ELASTIC SCATTERING BY DILUTE, IDEAL, POLYMER SOLUTIONS: II. EFFECTS OF HYDRODYNAMIC INTERACTIONS

E. DUBOIS-VIOLETTE and P.-G. de GENNES

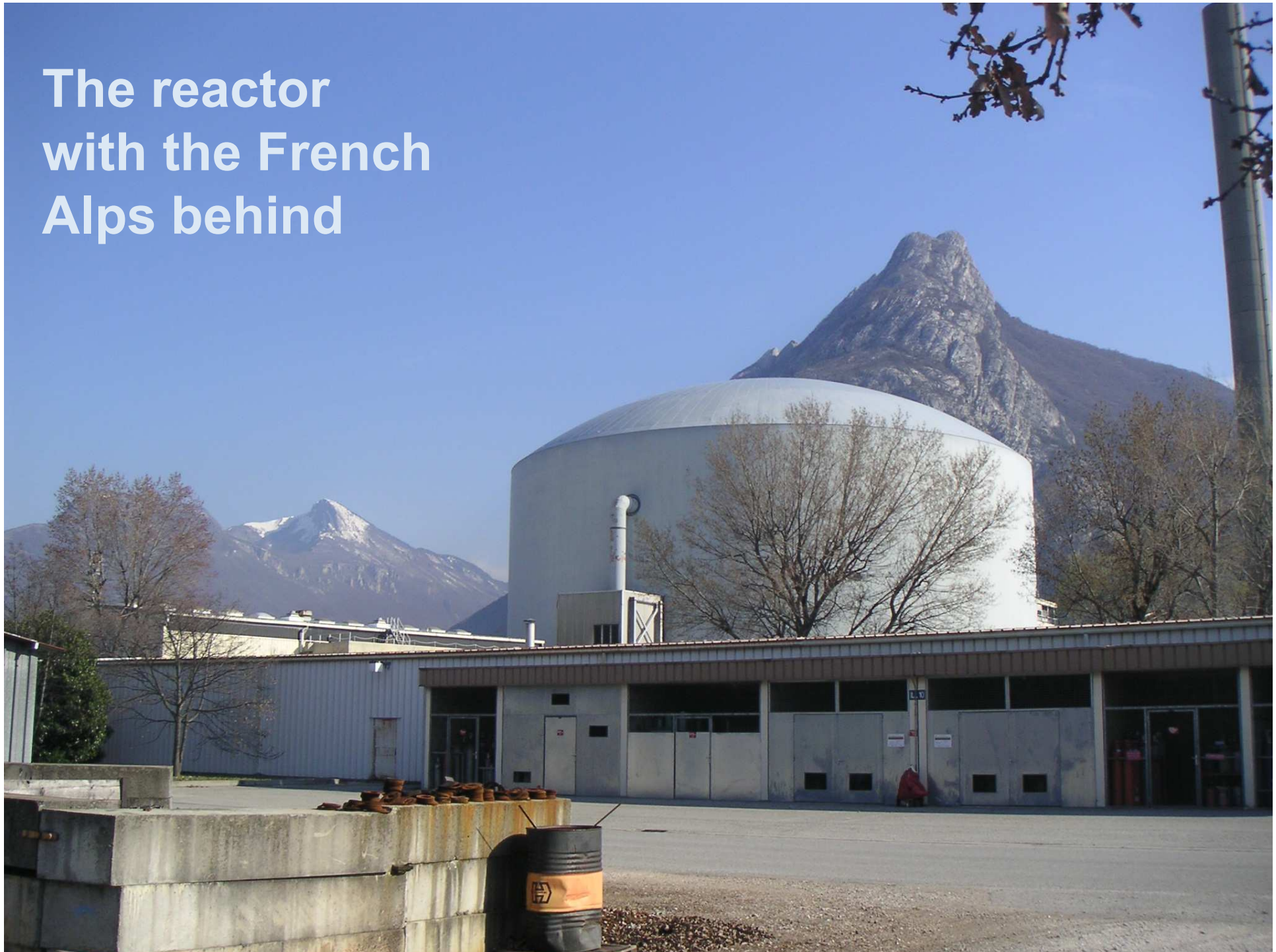
*Laboratoire de Physique des Solides**
Faculté des Sciences d'Orsay, 91 - ORSAY, France

(Received 21 February 1967)

Abstract

Each moving unit of a long, flexible, molecule induces in the surrounding solvent a velocity field which reacts on the motion of other segments. This long-range hydrodynamic interaction modifies strongly the dynamical form factor $S(\mathbf{q}\omega)$ at low frequencies ω and small scattering vectors \mathbf{q} . For neutron scattering ($qR_G \gg 1$, where R_G is the radius of gyration of the polymer), the frequency width $\Delta\omega_q$ of $S(q\omega)$ at fixed q becomes proportional to q^3 (for an ideal coil). Also the effect of stretching the molecule becomes more dramatic, since stretching greatly reduces the hydrodynamic interactions.

The reactor
with the French
Alps behind



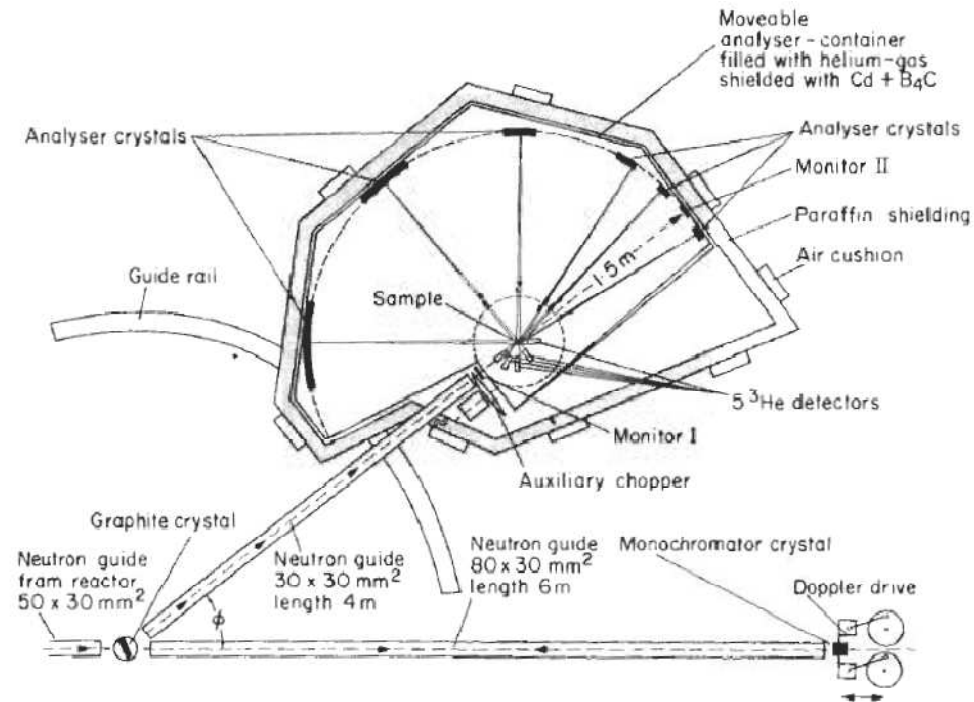


Figure 2.6 The back-scattering spectrometer (IN10) at HFR Grenoble

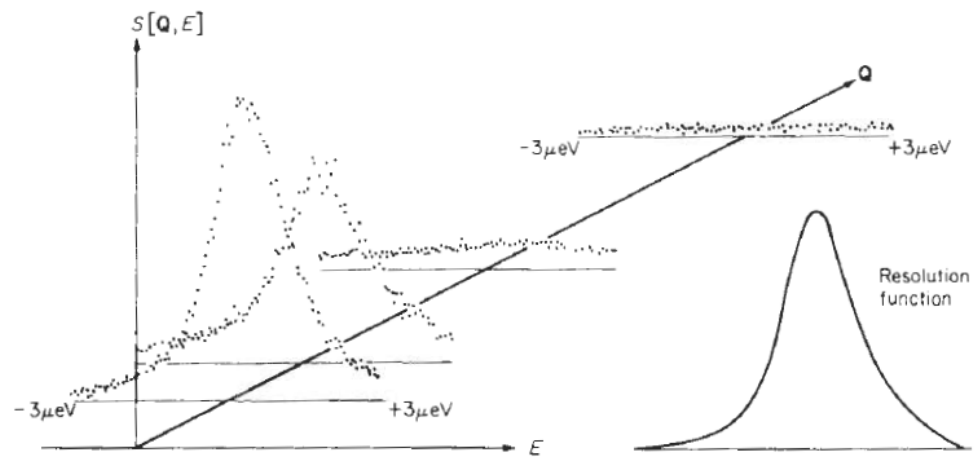
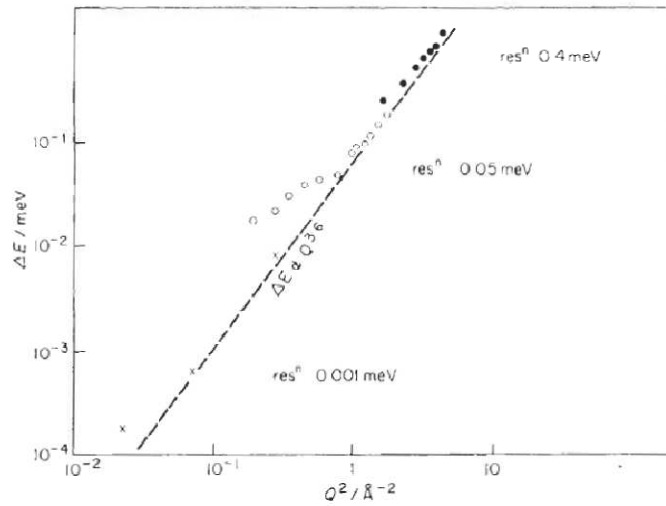
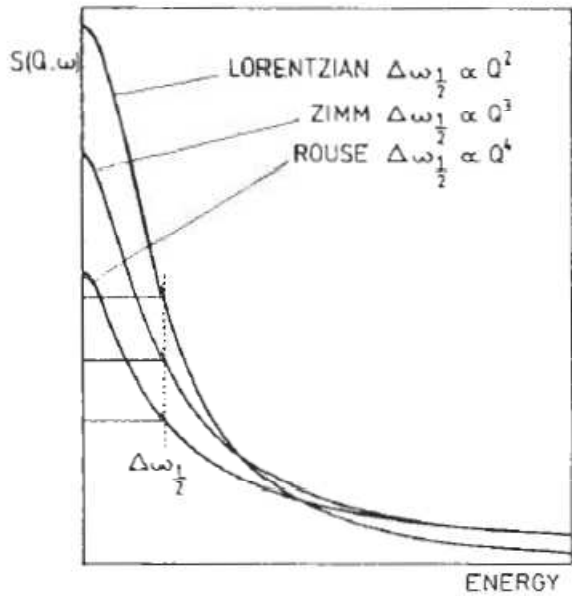


Figure 2.7 Normalized quasi-elastic scattering from polydimethylsiloxane shown on a 3-coordinate plot at four values of Q ($0.15, 0.27, 0.57, \text{ and } 0.97 \text{ \AA}^{-1}$). At the right-hand side the resolution function of the machine is shown on the same scale



Resolution problem

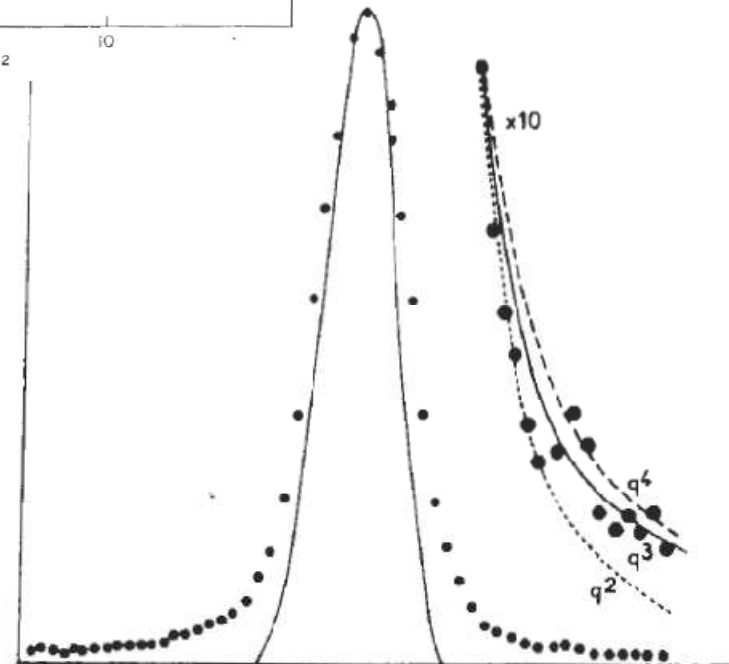
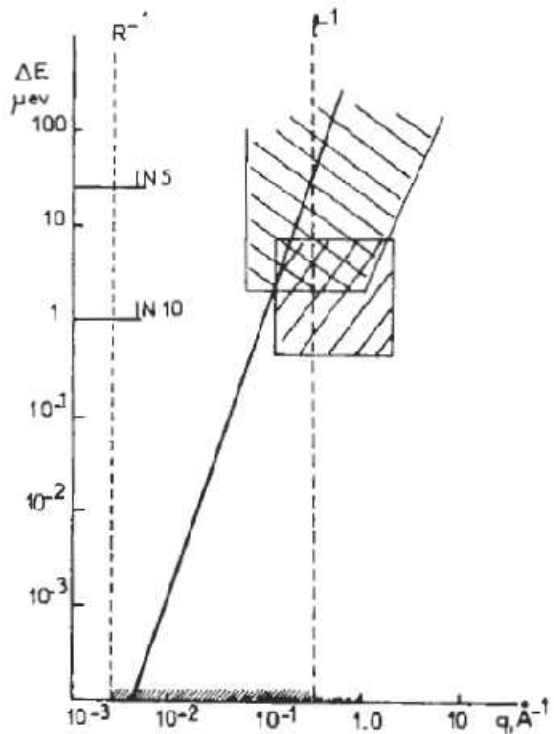
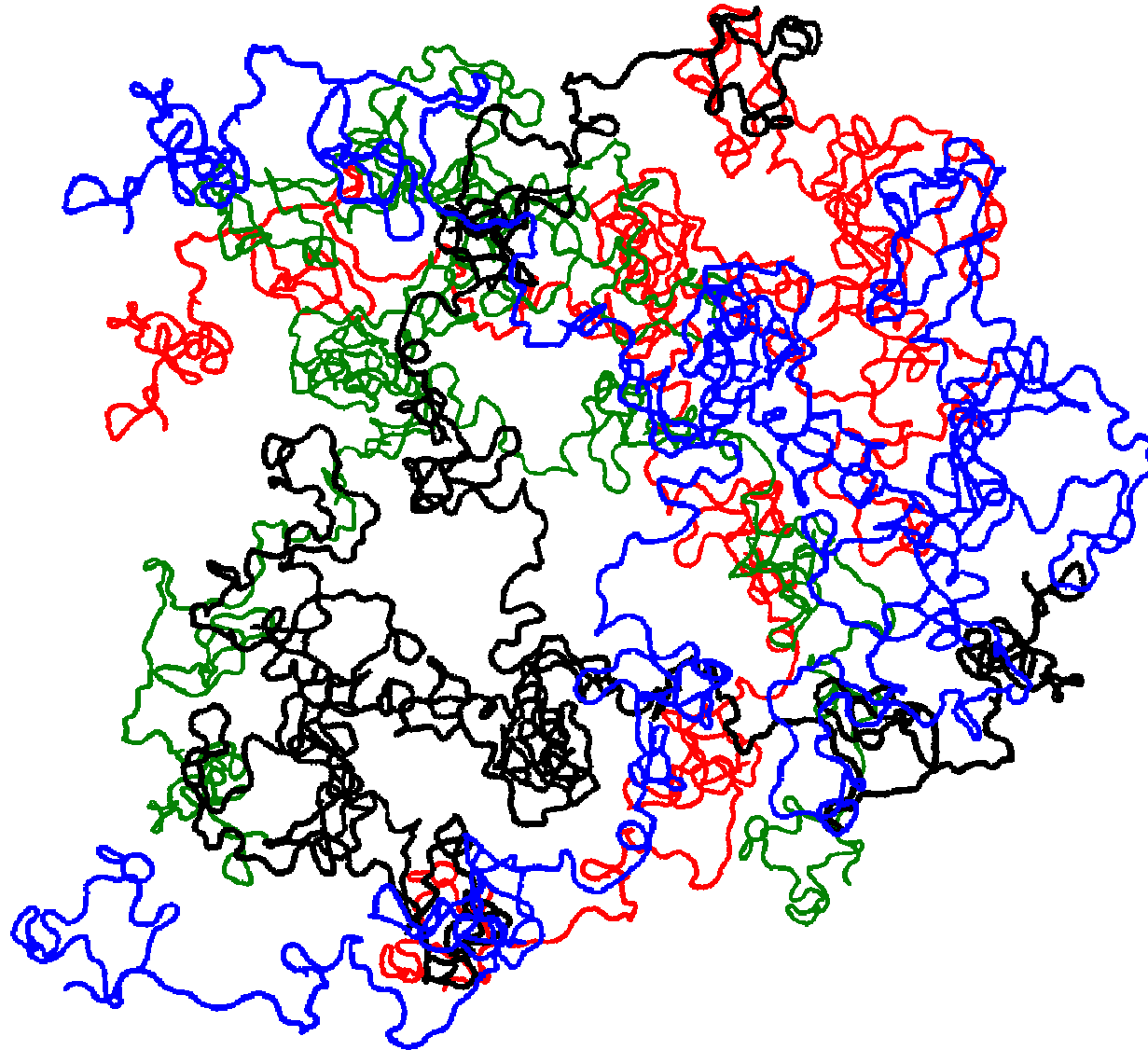
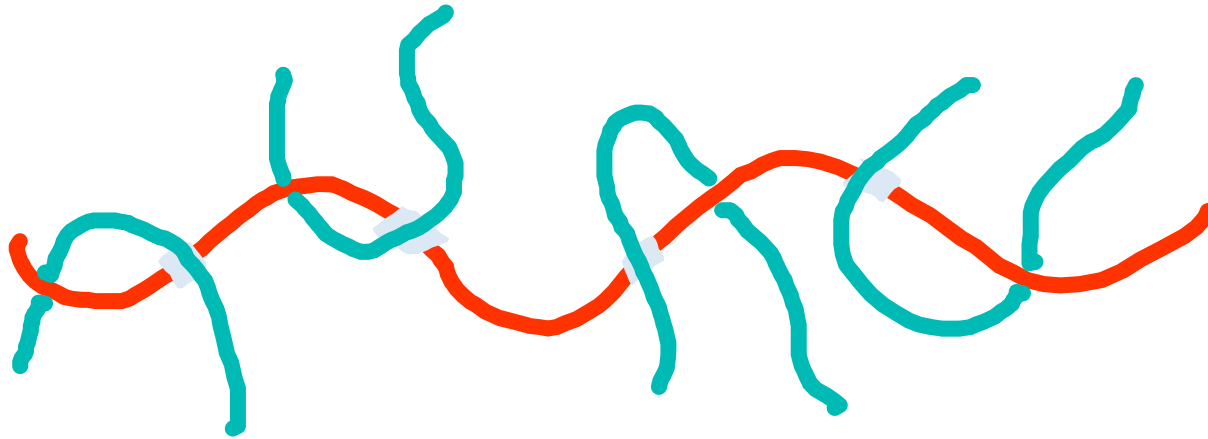


Fig. 2. An observed broadening (PTHF on IN 5 at $q = 0.25 \text{ \AA}^{-1}$, $\theta = 23^\circ$) together with the instrument profile. Enlarged in the wings are the best fit calculated line shapes for $\beta = 2$ ($R = 2.48$), $\beta = 3$ ($R = 1.43$) and $\beta = 4$ ($R = 2.91$).

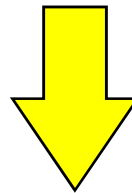
Entangled polymers – many random walks



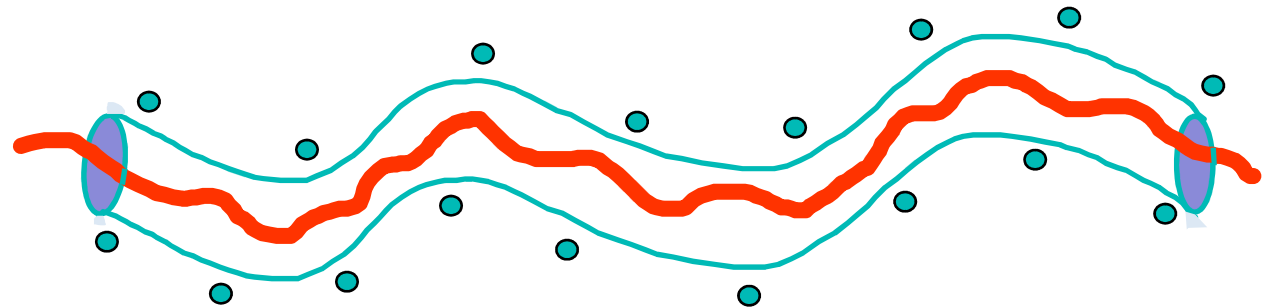
The Tube Model



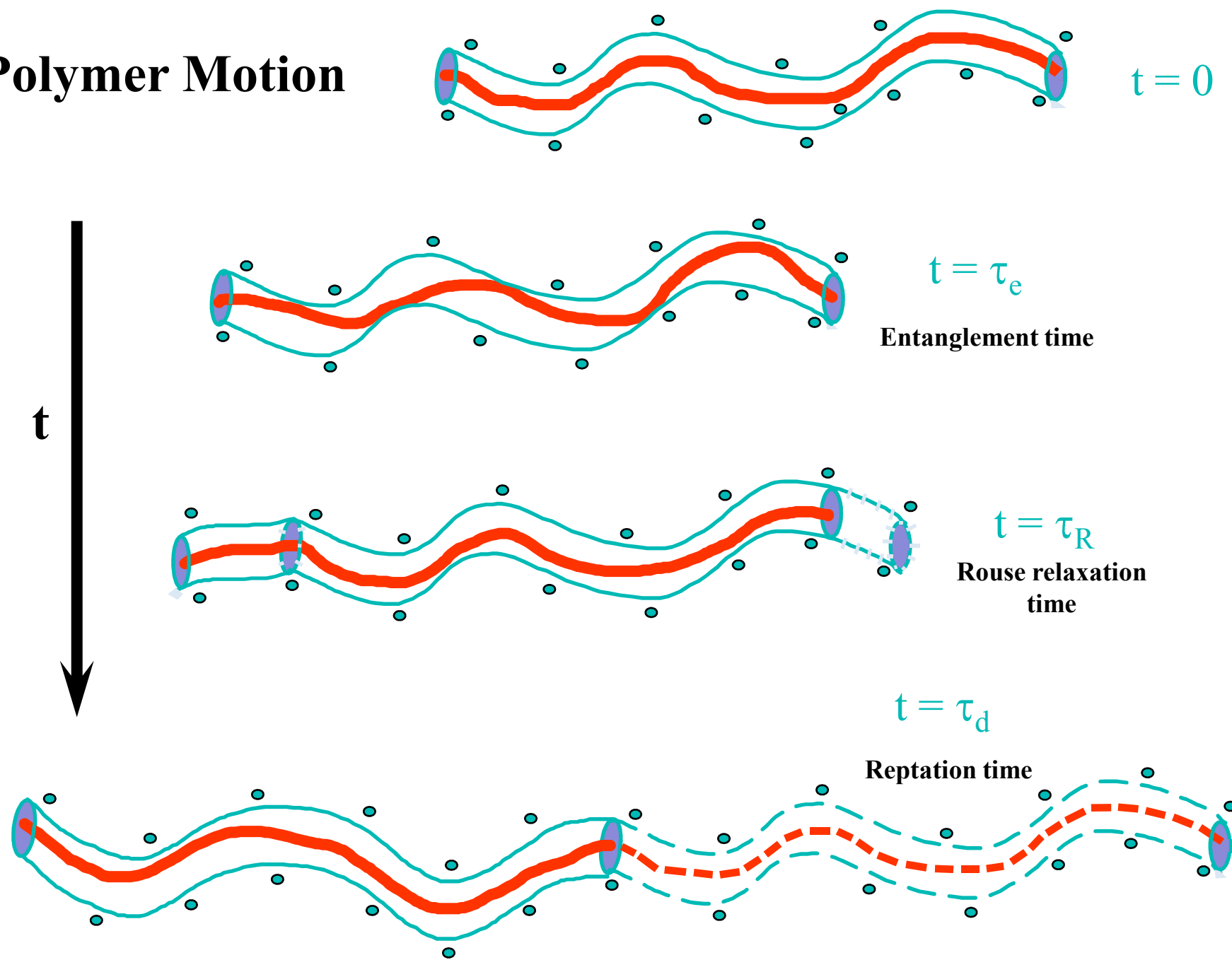
Polymer chains in the melt



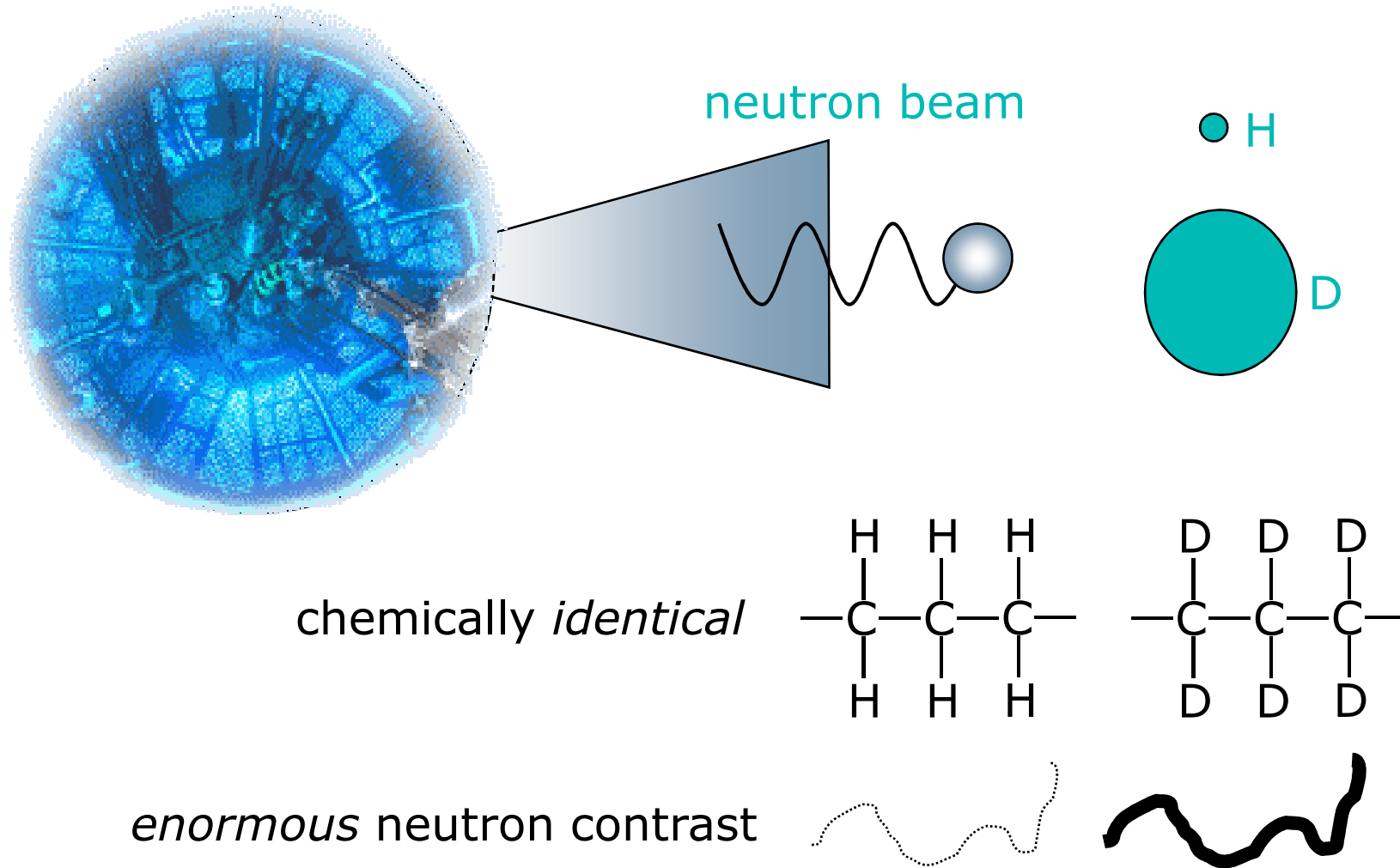
Each chain can be considered to be constrained within a tube



Polymer Motion

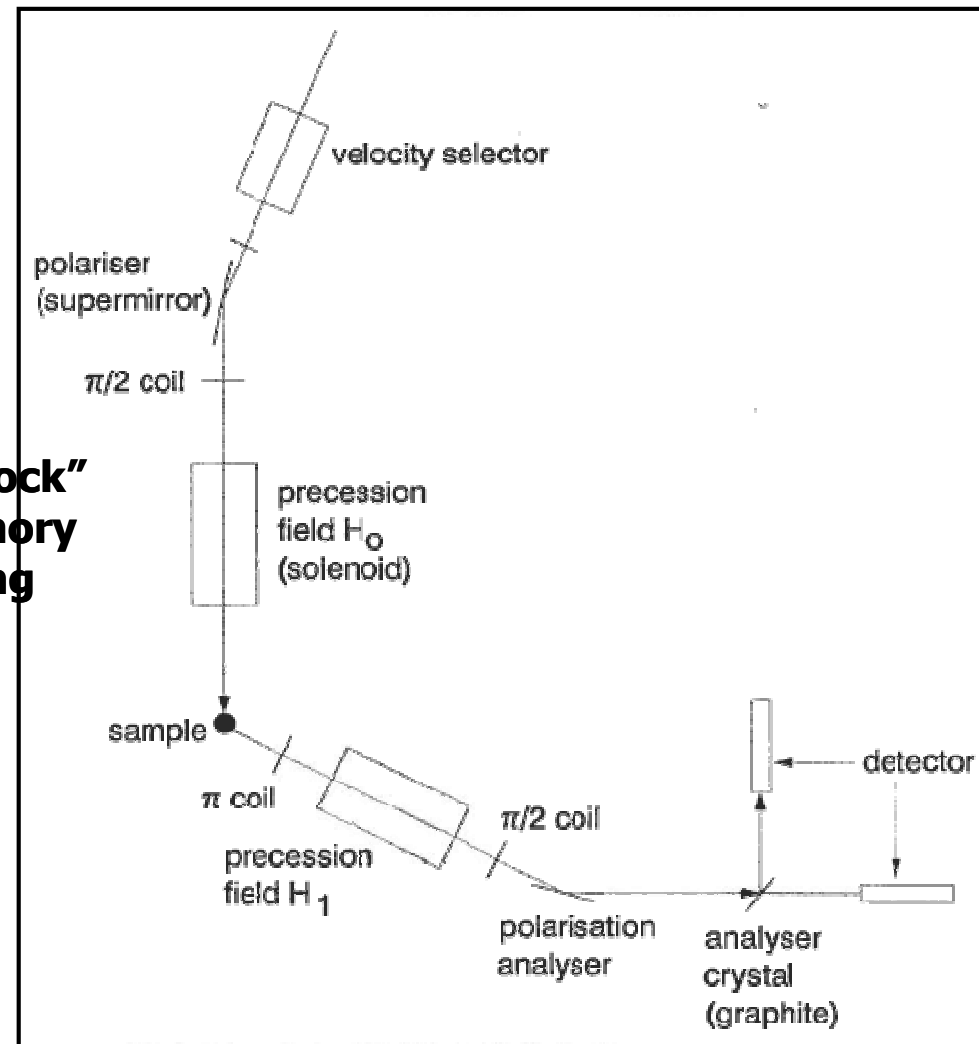


Neutron scattering



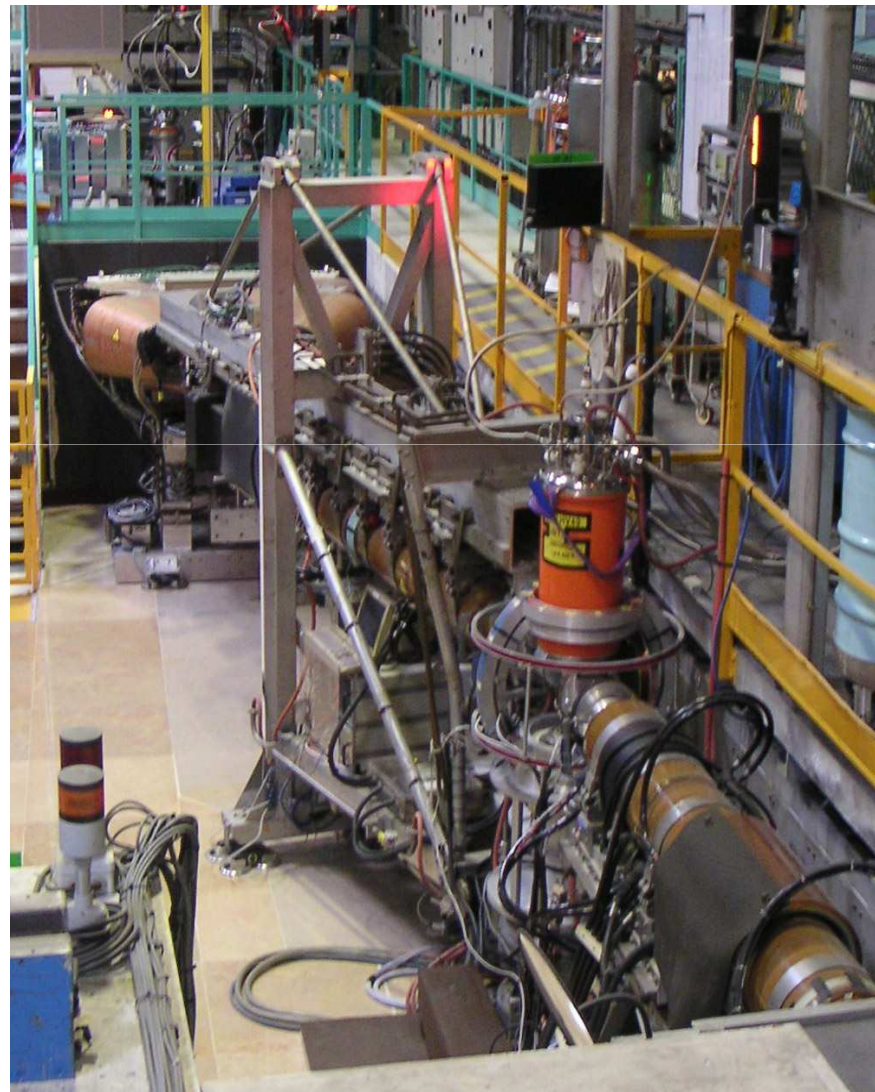
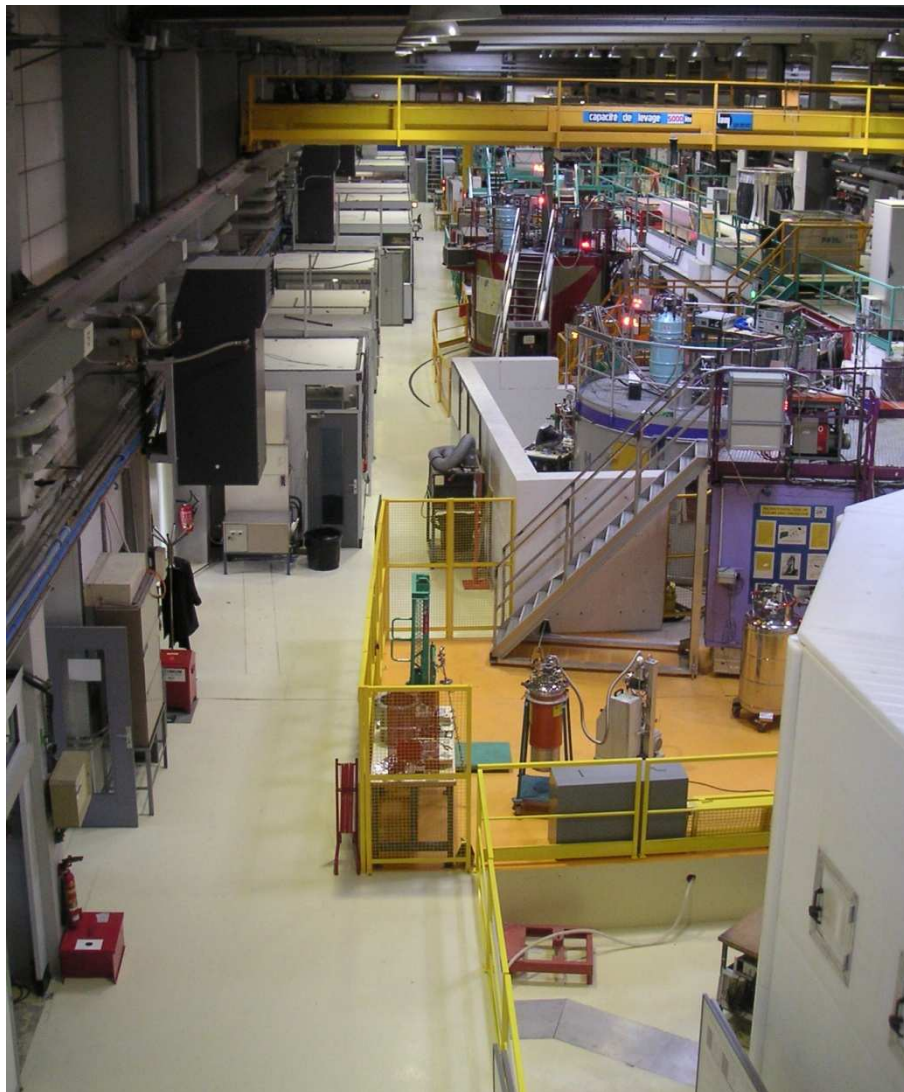
Neutron spin echo spectrometer IN11 (ILL, Grenoble)

Spin-echo uses the rotation of the neutron in a magnetic field as a "clock" to measure time during which memory of previous position of the scattering nuclei decays



neutron beam polarization, when normalized against a purely elastic scatterer (e.g., glassy polystyrene) is directly proportional to the cosine Fourier transform of the coherent scattering law, $S_{\text{coh}}(Q, \omega)$; i.e., the intermediate scattering law, or time correlation function, $S_{\text{coh}}(Q, t)$ is measured directly.

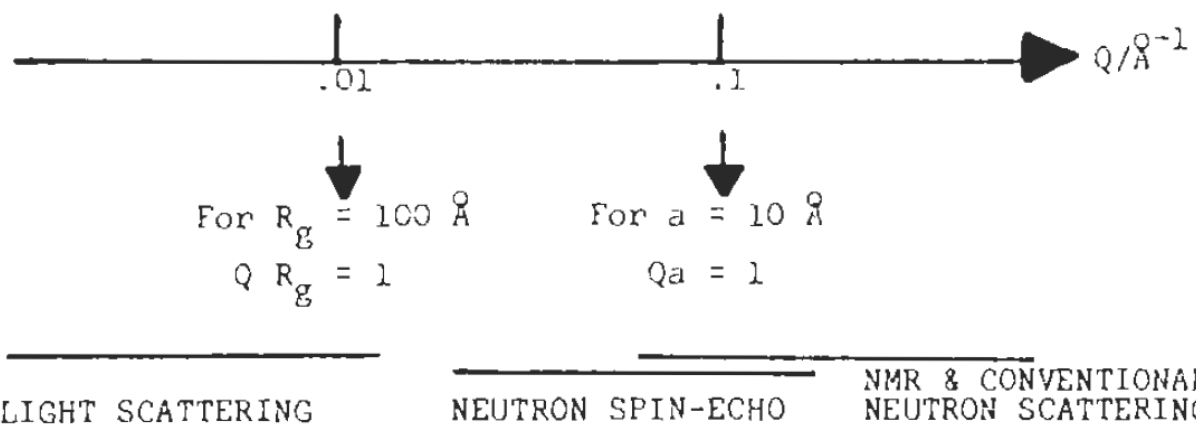
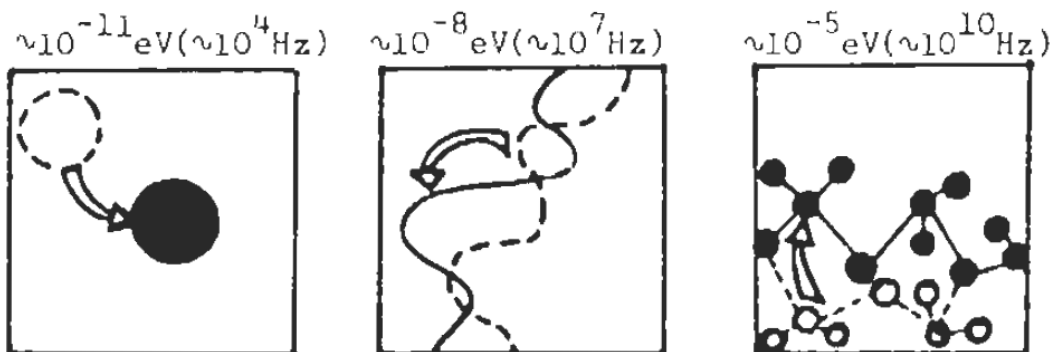
Large apparatus to investigate shape, size, organisation and motion of molecules



What are the advantages of neutron spin echo?

- It is highest energy resolution QENS technique
- It is a coherent scattering technique so we can exploit the SANS signal from labelled molecules
- It uses a highly collimated beam so we can measure at low q values – ie over reasonable spatial distances
- It measures the time FT of the normal $S(q,E)$ correlation function. In energy space this signal is a convolution of the energy spread in the incident beam and the signal from the sample. The FT of a convolution is a product. Hence the ***resolution function can be divided out*** from the NSE signal leaving the pure sample $S(q,t)$

TYPICAL ENERGIES OF MOTION (& CORRESPONDING FREQUENCIES)



In particular Akcasu *et al.* show that the initial time dependence of $S_{\text{coh}}(\kappa, t)$ obtained as:

$$\Omega = \lim_{t \rightarrow 0} \frac{d(\ln S(\kappa, t))}{dt} \quad (1)$$

is given by:

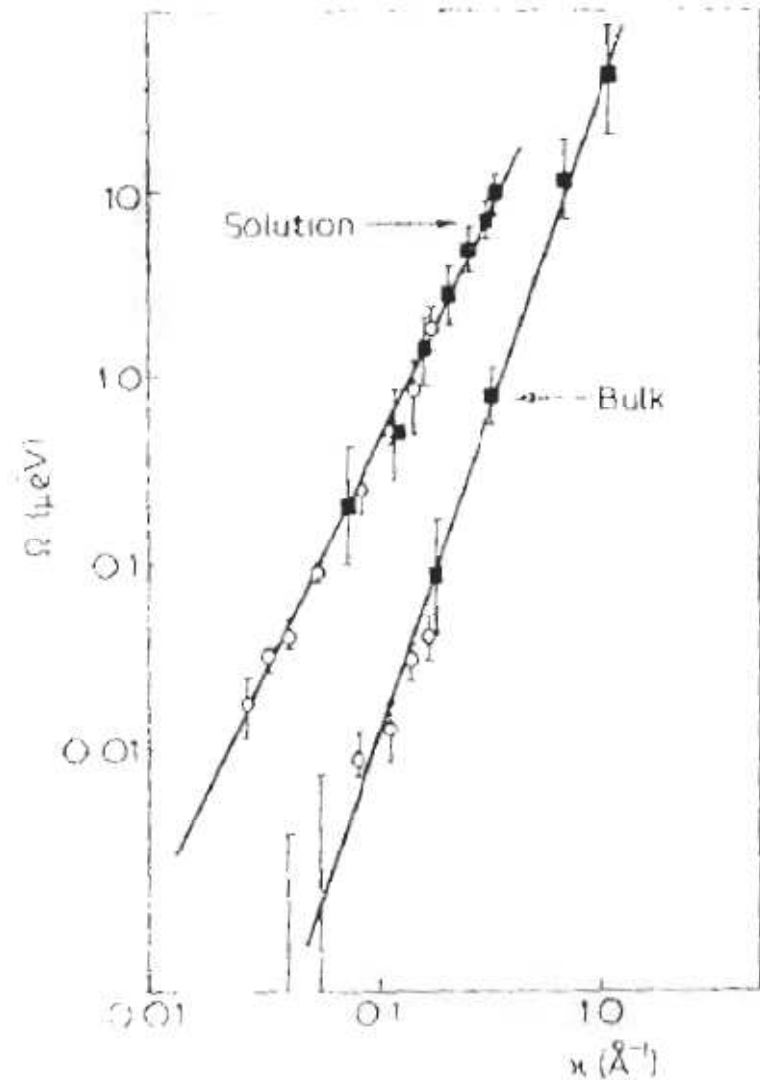
$$\Omega = \frac{1}{12} \frac{k_B T}{\zeta_0} \sigma^2 \kappa^4 \quad \text{s}^{-1} \quad (2)$$

where ζ_0 is a friction factor per step length σ .

The corresponding equation for dilute solution, where hydrodynamic effects are important is:

$$\Omega = \frac{1}{6\pi} \frac{k_B T}{\eta} \kappa^2 \quad \text{s}^{-1} \quad (3)$$

i.e. the κ dependence is slower and only the solvent viscosity determines the prefactor.



J. Phys. France **42**, 735-740 (1981)
DOI: 10.1051/jphys:01981004205073500

Coherent scattering by one reptating chain

P.G. De Gennes

Physique de la Matière Condensée, Collège de France, 75231 Paris Cedex 05, France

Résumé

On analyse la structure de la fonction de diffusion cohérente $S(q,t)$ pour une chaîne polymérique deutérée se déplaçant dans un fondu de chaînes enchevêtrées, chimiquement identiques mais non deutérées. Le domaine intéressant correspond à des longueurs d'onde $2\pi/q$ plus petites que la taille globale de la chaîne (R_0) mais plus grandes que la distance D entre points d'enchevêtrement. Dans ce domaine, nous sommes conduits à une forte autocritique : les résultats sont beaucoup plus complexes que nous ne l'avions imaginé dans un travail antérieur [1]. La fonction $S(q,t)$ se sépare en : a) une partie $S_1(q,t)$ qui décrit des fluctuations locales dans le tube, et qui relaxe relativement vite; b) une partie $S_c(q,t)$ qui est de plus grande amplitude, et qui ne décroît que très lentement (avec pour temps caractéristique le temps de reptation globale T_{rep}). Dans la référence [1] nous avons postulé une seule fréquence caractéristique ($1/\tau_q \sim q^6$). Il s'avère que cet $1/\tau_q$ est seulement la moyenne pondérée des deux fréquences physiques associées à S_1 et S_c .

Abstract

We discuss the time dependent correlation functions $S(q,t)$ for one deuterated polymer chain, moving inside an entangled melt of chemically identical, protonated, chains. The region of interest corresponds to wave-vectors q such that $D^{-1} \gg q \gg R_0^{-1}$ where D is the tube diameter and R_0 the overall chain size. In this regime the results disagree strongly with our earlier prediction [1]. We find that the function $S(q,t)$ breaks up into two parts. One part [$S_1(q,t)$] describes the local fluctuations of « kinks » inside the tube and relaxes relatively fast (characteristic time $\sim q^{-4}$). The other part [$S_c(q,t)$], with much larger amplitude, describes a slow, global creep of the chain inside its tube, associated with the tube diffusivity D_t . The characteristic time for this creep process is independent of q , and is the overall reptation time T_{rep} . In reference [1] a single characteristic rate $1/\tau_q \sim q^6$ was constructed for each q vector : this turns out to be the weighted average of the two physical relaxation rates.

(a) $Q < R_g^{-1}$, diffusion regime:

$$S'(Q, t) = \exp(-\Omega_m t) \quad (3)$$

$$\Omega_m = D_m Q^2 \quad (4)$$

where D_m is the centre-of-mass diffusion coefficient.

(b) $R_g^{-1} < Q < \sigma^{-1}$, 'universal' (intermediate) regime: in the Rouse limit⁴

$$S'(Q, t) = \int_0^\infty du \exp \left[-u - (\Omega_R t)^{1/2} g \left(\frac{u}{(\Omega_R t)^{1/2}} \right) \right] \quad (5a)$$

$$g(y) = \frac{2}{\pi} \int_0^\infty dx \frac{1 - \exp(-x^2)}{x^2} \cos(yx) \quad (5b)$$

$$\Omega_R = -\lim_{t \rightarrow 0} \frac{d}{dt} S'(Q, t) = \frac{1}{12} \frac{kT\sigma^2}{f} Q^4 \quad (6)$$

where f is a segmental friction coefficient and k and T are the Boltzmann constant and temperature, respectively. The long-time asymptotic behaviour of the Rouse chain is given by

$$S'(Q, t) \approx \exp \left(-\frac{2}{\sqrt{\pi}} (\Omega_R t)^{1/2} \right). \quad (7)$$

For the entangled melt ($R_g^{-1} < Q \ll D^{-1}$) de Gennes¹⁷ suggested, in the framework of the reptation model, an overall correlation function of one chain which can be written as:

$$S'(Q, t) = \frac{Q^2 D^2}{36} S'_{\text{local}}(Q, t) + \left(1 - \frac{Q^2 D^2}{36} \right) S'_{\text{creep}}(Q, t) \quad (8a)$$

$$S'_{\text{local}}(Q, t) = \exp(\Omega_R t) [1 - \text{erf}(\Omega_R t)^{1/2}] \quad (8b)$$

$$S'_{\text{creep}}(Q, t) = \frac{8}{\pi^2} \exp \left(-\frac{t}{T_{\text{rep}}} \right) \left\{ 1 + \sum_{n=3}^{\text{odd}} \frac{1}{n^2} \left(\frac{\pi^2}{8} \right)^{n^2-1} \times \left[\frac{8}{\pi^2} \exp \left(-\frac{t}{T_{\text{rep}}} \right) \right]^{n^2-1} \right\} \quad (8c)$$

where T_{rep} is the reptation time.

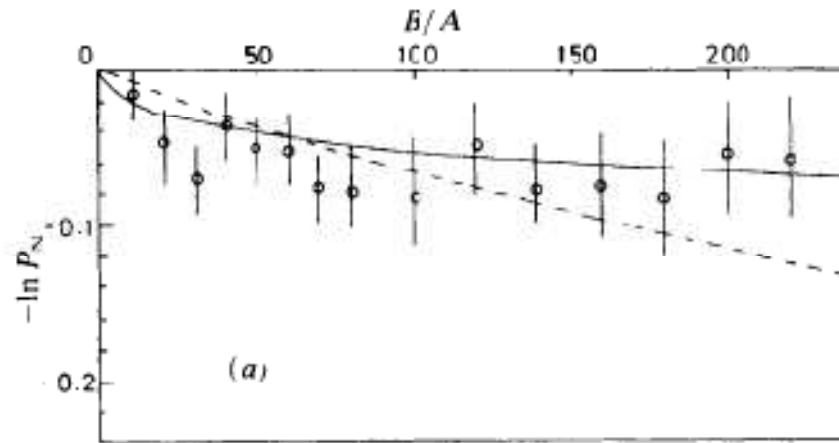
Effects of Entanglements on the Single-chain Motion of Polymer Molecules in Melt Samples Observed by Neutron Scattering

BY JULIA S. HIGGINS* AND JAAN E. ROOTS†

Department of Chemical Engineering and Chemical Technology,
Imperial College, London SW7 2BY

Received 15th October, 1984

The motion of single molecules of polytetrahydrofuran in melt samples of deuterated polytetrahydrofuran has been observed using high-resolution quasi-elastic neutron scattering (the neutron spin-echo technique). Comparison of results for two systems in which the matrix of deuterated molecules surrounding the observed molecules is either well above or well below the entanglement molecular weight shows clearly the effects of molecular entanglements on the observed correlation functions. The form of these correlation functions agrees with the theoretically predicted behaviour for entangled systems and allows a value for the average distance between entanglements of 30 Å to be extracted.



Reptation

Rouse

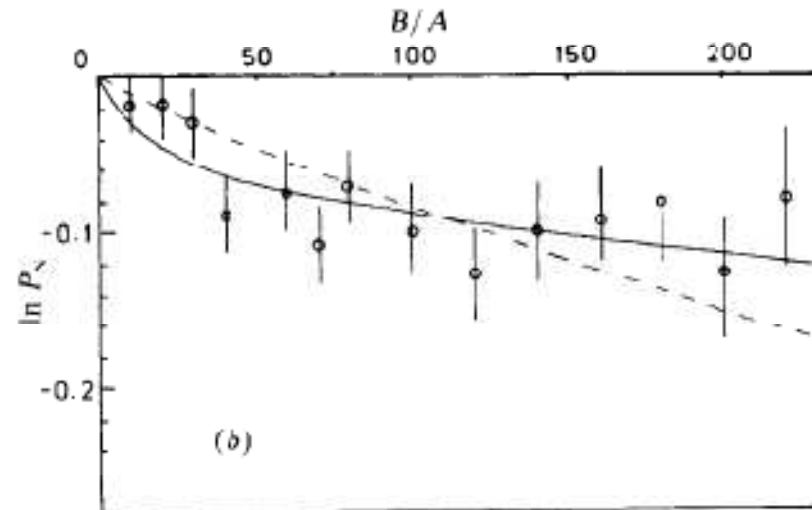


Fig. 5. Comparison of fits of eqn (5a) (dashed line) and eqn (8a) (solid line) for H/H (see text). $Q/\text{\AA}^{-1}$: (a) 0.08 and (b) 0.09.

Rouse

$$S'(Q, t) = \int_0^\infty du \exp \left[-u - (\Omega_R t)^{1/2} g \left(\frac{u}{(\Omega_R t)^{1/2}} \right) \right] \quad (5a)$$

Reptation

$$S'(Q, t) = \frac{Q^2 D^2}{36} S'_{\text{rept}}(Q, t) + \left(1 - \frac{Q^2 D^2}{36} \right) S'_{\text{creep}}(Q, t) \quad (8a)$$

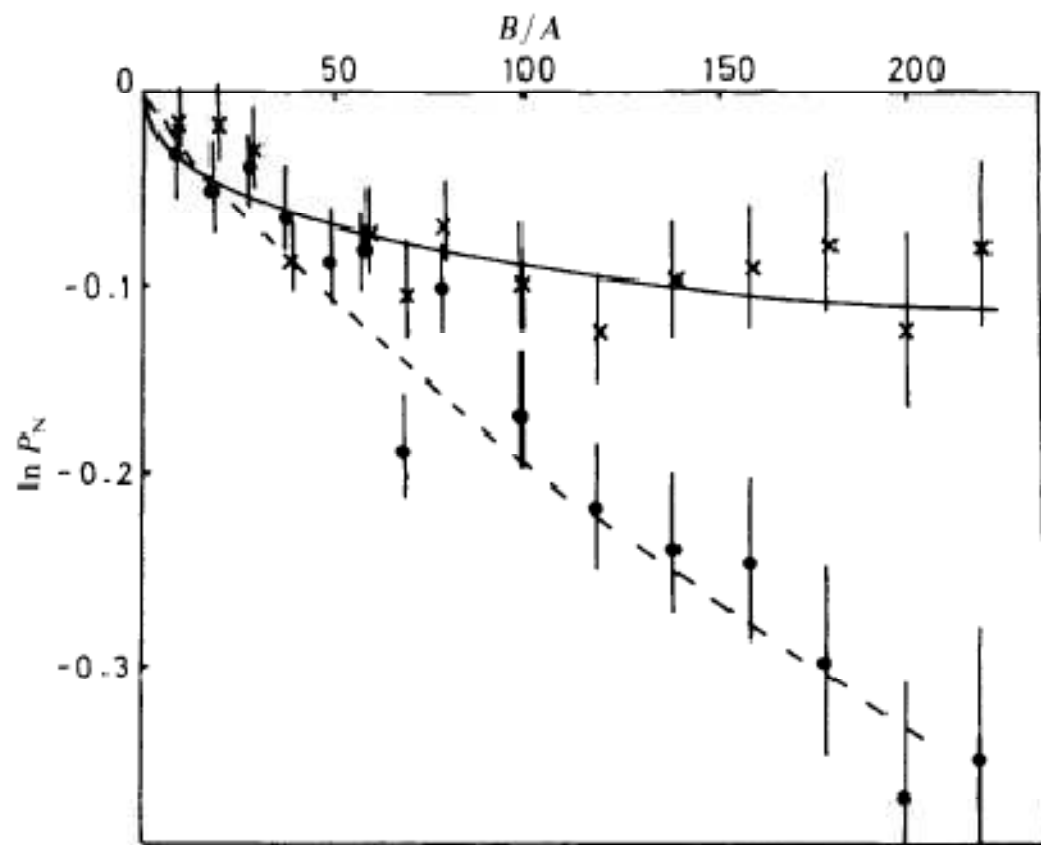


Fig. 4. Comparison of the correlation functions for the samples H/L and H/H at $Q = 0.09 \text{ \AA}^{-1}$. The dashed line is the best fit of eqn (5a). The solid line is the fit of eqn (8a) using the value of Ω_R obtained for the sample H/L (*cf.* the main text). ●, H/L and ×, H/H.

$$S'(Q, t) = \frac{Q^2 D^2}{36} S'_{\text{local}}(Q, t) + \left(1 - \frac{Q^2 D^2}{36}\right) S'_{\text{creep}}(Q, t) \quad (8a)$$

Scientists need good luck!

Two parameters are important in deciding whether the effect of entanglements can be seen in a spin echo experiment, *Rouse time AND tunnel width, D*

We had all concentrated on the *energy resolution* question and hence the Rouse time. This *implied PDMS* would be the polymer of choice.

For us however the *choice* of polymer was driven by *necessity!*

We needed an *h/d mixture* to give the coherent scattering from single chains

To reduce the incoherent signal we needed a mix *90% deuterated*.

Such polymers are expensive or unobtainable! BUT d-tetrahydrofuran is an *NMR solvent* and is *CHEAP!* It is not difficult to polymerise.

Our chemists made the d and h polymers for us – in high and low Mw samples.

No-one had measured the rheology or obtained the *tunnel width for PTHF* – it was not an important polymer!

From the *neutron experiments D* turned out to be *around 30A* like PE and much smaller than D for PDMS (which is around 80A like PS)

Table 3. Long-time limit of scattering function and calculated values of $\langle r_E^2 \rangle^{1/2}$ [eqn (9)]

$Q/\text{\AA}^{-1}$	$S(Q, \infty)$	$\langle r_E^2 \rangle^{1/2}/\text{\AA}$
0.079	0.935 ± 0.02	30 ± 2
0.092	0.918 ± 0.035	27 ± 3
0.106	0.847 ± 0.02	28 ± 1

There are currently very few viscoelastic data for PTHF available in the literature. However, recent measurements²⁸ of the plateau modulus G_N^0 allow a value of D to be calculated using Doi-Edwards theory.¹⁶ The value obtained is 31.5 Å, in very good agreement with the neutron-scattering result.

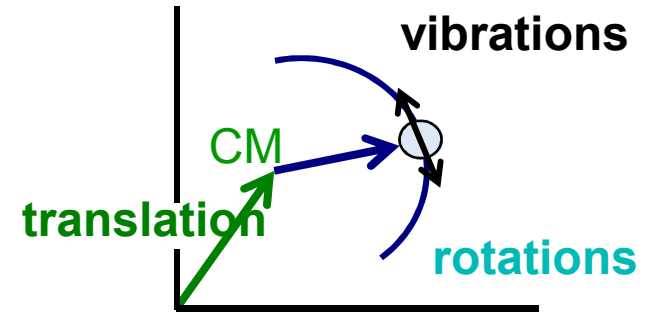
²⁸ D. Pearson, to be published.

²⁹ W. Graessley, personal communication.

So where did QENS from polymers develop?

- Higher resolution spin echo experiments with improved statistics and longer time scales from different polymers including PDMS
- Exploration of different molecular architectures in spin echo, as well as mixtures
- Exploitation of the time domain to remove the convolution problem— even from energy domain experiments
- Comparison of molecular modelling results with QENS experiments
- Construction of more spin-echo spectrometers at neutron sources in Europe, Japan and USA

single-particle dynamics



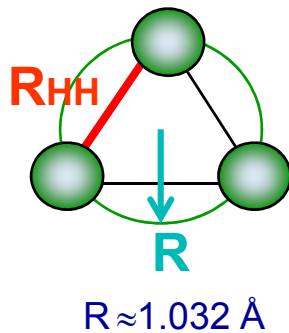
motion decomposition

$$I_{self}(Q, t) = \frac{1}{N} \sum_i \langle e^{iQ \cdot [V(t) - V(0)]} \rangle \langle e^{iQ \cdot [T(t) - T(0)]} \rangle \langle e^{iQ \cdot [R(t) - R(0)]} \rangle$$

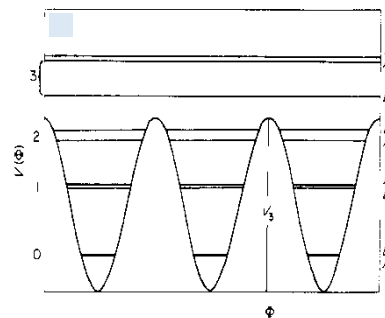
CM translation: frozen for polymers $T \ll T_g$.

Proton delocalisation: DW factor: $e^{-\frac{1}{3}Q^2 \langle u^2 \rangle}$

Rotations: **Methyl protons 3-fold jumps**



3-fold CH₃ potential



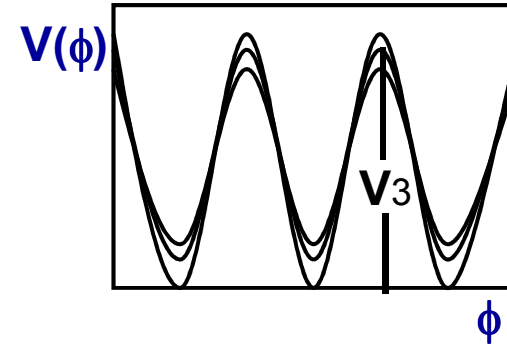
$$S_{rot}(Q, \omega) = A_0(Q)\delta(\omega) + A_1(Q) \frac{1}{\pi} \frac{3/2\tau}{(3/2\tau)^2 + \omega^2}$$

with

$$\begin{cases} A_0(Q) = \frac{1}{3} [1 + 2j_0(Qr\sqrt{3})] \\ A_1(Q) = 1 - A_0(Q) \end{cases}$$

distribution $\tau_{\text{correlation}}$

glassy polymers: no single relaxation time
 variety local | **intra-** molecular environments
 | **inter-**



(Gaussian) distribution of potential barriers:

$$g(E_i) = \frac{1}{\sigma_E \sqrt{2\pi}} e^{-\frac{(E_i - E_0)^2}{2\sigma_E^2}} \quad \text{if } \Gamma = \Gamma_0 e^{-\frac{E_A}{RT}}$$

(log-Gaussian) distribution of reorientation times:

$$g(\ln \Gamma_i) = \frac{1}{\sigma \sqrt{2\pi}} e^{-\frac{\ln^2(\Gamma_i/\Gamma_0)}{2\sigma^2}} \quad \begin{array}{l} E_0: \text{average barrier height} \\ \sigma: \text{distribution width} \end{array}$$

Dynamic structure factor: $S_{\text{rot}}(Q, \omega) = A_0(Q)\delta(\omega) + A_1(Q) \sum_{i=1}^N g_i L_i(\omega)$

Rotation of Methyl Side Groups in Polymers: A Fourier Transform Approach to Quasielastic Neutron Scattering. 1. Homopolymers

V. Arrighi* and J. S. Higgins

Chemical Engineering Department, Imperial College, London SW7 2BY, U.K.

A. N. Burgess

ICI Chemicals and Polymers, Runcorn WA7 4QD, U.K.

W. S. Howells

ISIS Pulsed Source, Rutherford Appleton Laboratory, Chilton, Didcot OX11 0QX, U.K.

*Received July 5, 1994; Revised Manuscript Received December 27, 1994**

ABSTRACT: The rotational motion of the ester methyl group in poly(methyl methacrylate) (PMMA) was investigated using quasielastic neutron scattering (QENS). A comparison between our results and the QENS data reported in the literature for PMMA-*d*₅ indicates that the amount of quasielastic broadening is highly dependent upon the energy resolution of the spectrometer. This anomalous behavior is here attributed to the method of analysis, namely, the use of a single rotational frequency. Such a procedure leads to a non-Arrhenius temperature dependence, to a temperature-dependent elastic incoherent structure factor, and to values of rotational frequency which are resolution dependent. We propose an alternative approach to the analysis of the QENS data which accounts for the existence of a distribution of rotational frequencies. The frequency data are Fourier transformed to the time domain, and the intermediate scattering function is fitted using a stretched exponential or Kohlraush–Williams–Watts function. The excellent overlap between data from different spectrometers leaves no doubt on the adequacy of our procedure. Measurements of the ether methyl group rotation in poly(vinyl methyl ether) (PVME) are also reported. The PVME data confirm that the behavior observed for PMMA-*d*₅ is likely to be a common feature to all polymeric systems.

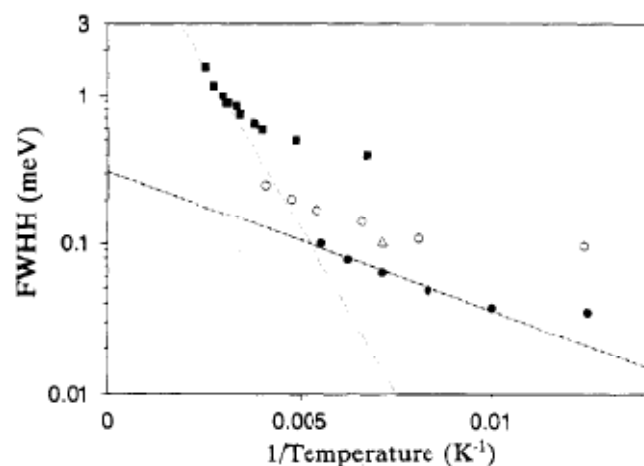


Figure 1. Full width at half-height (fwhh) versus inverse temperature for PMMA- d_5 measured: (○) on MIBEMOL, this work; (△) on QENS, this work; (■) on IN5 and IN6 by Gabrys et al.;⁶ (●) on IRIS.¹³ All data were analyzed using a single Lorentzian line convoluted with the instrumental resolution on top of a flat background. The lines indicate a fit to the high- and low-temperature data.

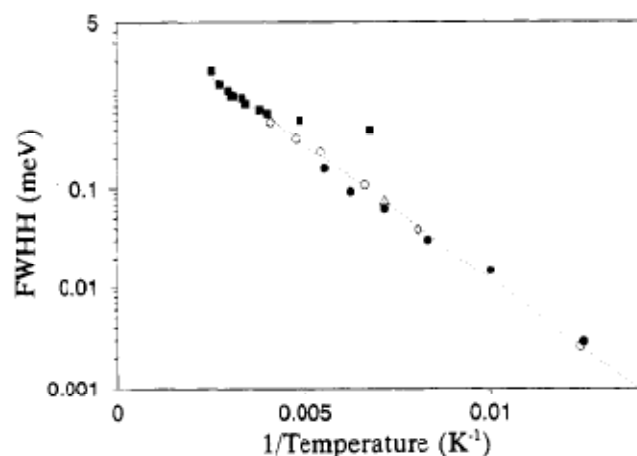


Figure 11. Temperature dependence of fwhh or $2\tau_c$ (in meV) of PMMA- d_5 measured from $I(Q,t)$: (○) on MIBEMOL, this work; (△) on QENS, this work; (●) on IRIS, this work; (■) comparison with fwhh from IN5, and IN6 measured by Gabrys et al. (the frequency data were analyzed using a single Lorentzian line). The dotted line shows a fit through the experimental points.

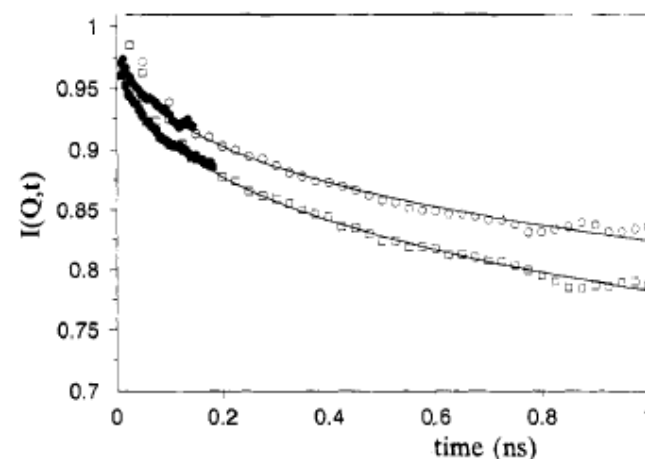


Figure 10. Intermediate scattering function of PMMA- d_5 at 80 K and $Q = 1.32 \text{ \AA}^{-1}$ as measured on (○) IRIS and (●) MIBEMOL and at $Q = 1.64 \text{ \AA}^{-1}$ as measured on (■) MIBEMOL and (□) IRIS. The lines indicate fits through the combined data using eq 13.

$$I(Q,t) = A_0(Q) + [1 - A_0(Q)] \exp\left(-\frac{t}{\tau_c}\right)^\beta \quad (13)$$

Self- and Collective Dynamics of Syndiotactic Poly(methyl methacrylate). A Combined Study by Quasielastic Neutron Scattering and Atomistic Molecular Dynamics Simulations

A.-C. Genix,^{*,†} A. Arbe,[‡] F. Alvarez,^{‡,§} J. Colmenero,^{†,‡,§} B. Farago,^{||}
A. Wischnewski,[⊥] and D. Richter[⊥]

ABSTRACT: We have investigated the molecular dynamics of syndiotactic poly(methyl methacrylate) well above the glass transition by combining quasielastic neutron scattering and fully atomistic computer simulations. The incoherent scattering measured by backscattering on a sample with deuterated ester methyl groups has revealed the single-particle motions of hydrogens in the main chain and in the α -methyl groups. Moreover, with neutron spin-echo experiments on the fully deuterated sample we have accessed the collective motions at the two first maxima of the structure factor. The simulated cell, which has been previously validated regarding the structural properties [Genix, A.-C.; et al. *Macromolecules* 2006, 39, 3947], shows a dynamical behavior that, allowing a shift in temperature, reproduces very accurately all the experimental results. The combined analysis of both sets of data has shown that: (i) The segmental relaxation involving backbone atoms deviates from Gaussian behavior. (ii) The dynamics is extremely heterogeneous: in addition to the subdiffusion associated with the α -process and the methyl group rotations, we have found indications of a rotational motion of the ester side group around the main chain. (iii) At a given momentum transfer and depending on the molecular groups considered, the time scales for collective motion are spread over about 1 order of magnitude, the correlations involving the main chain decaying much more slowly than those relating side groups. (iv) At the length scale characteristic for the overall periodicity of the system (that corresponding to the first structure factor peak), the experimentally observed collective dynamics relates to the backbone motions and is of interchain character; there, coherency effects are observed for all correlations, though side groups display weaker collectivity. (v) At the second structure factor peak, coherency remains only for correlations involving the main chains.

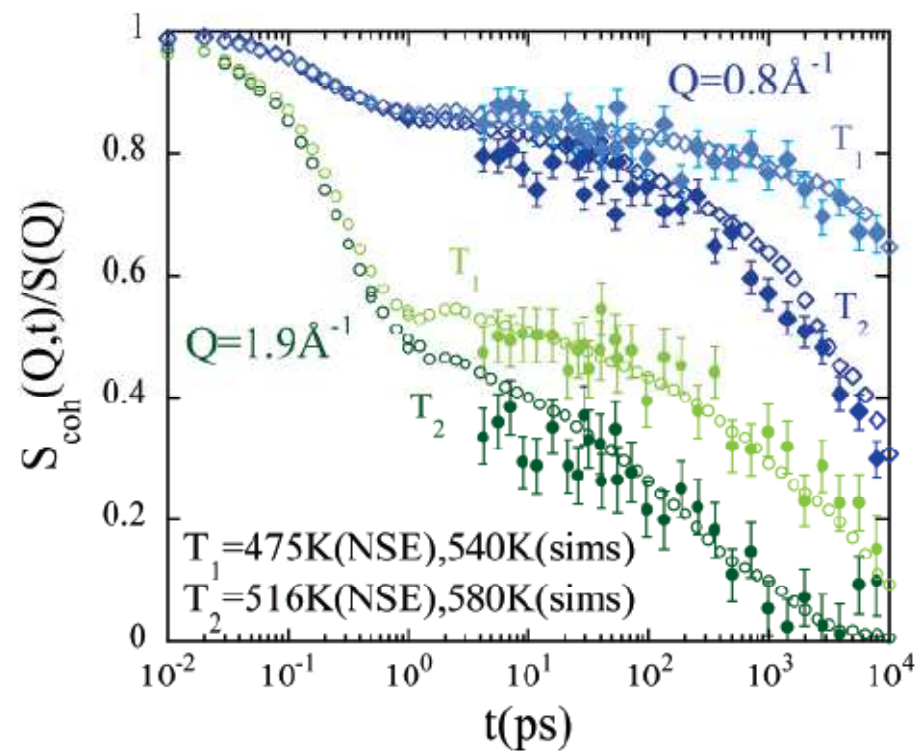


Figure 6. Dynamic structure factor of PMMA: simulation results (empty symbols) and IN11 results (full symbols) for $Q = 0.8 \text{ \AA}^{-1}$ (rhombs) and $Q = 1.9 \text{ \AA}^{-1}$ (circles). The amplitudes of the experimental data have been corrected for the band-pass of the spectrometer using the MD simulations results at $t = 0.2 \text{ ps}$.



Spin-echo spectrometer with time-of-flight and focusing option IN15

IN15 is a high energy and momentum resolution spin-echo spectrometer optimised for quasielastic small angle scattering. This instrument is developed and financed jointly by the ILL, FZ Jülich and HMI Berlin.



Spin-echo spectrometers

IN15

Applications & selected example

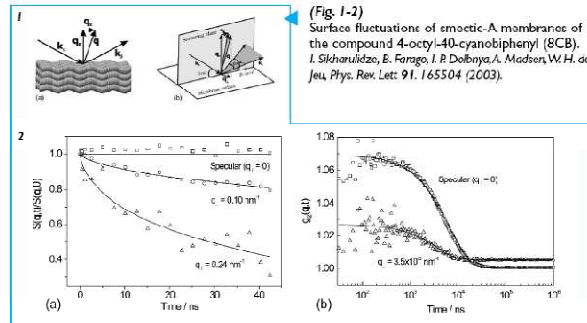


(Fig. 1-2) Surface fluctuations of emectic-A membranes of the compound 4-octyl-40-cyanobiphenyl (8CB). I. Siharulidze, B. Forago, I. P. Dolbnya, A. Madsen, W. H. de Jeu, *Phys. Rev. Lett.* **91**, 165504 (2003).

1 - Scattering geometry,
2 - (a) NSE (b) XPCS measurements.

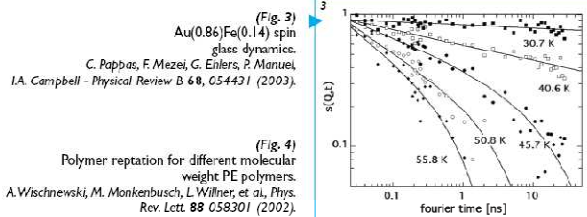
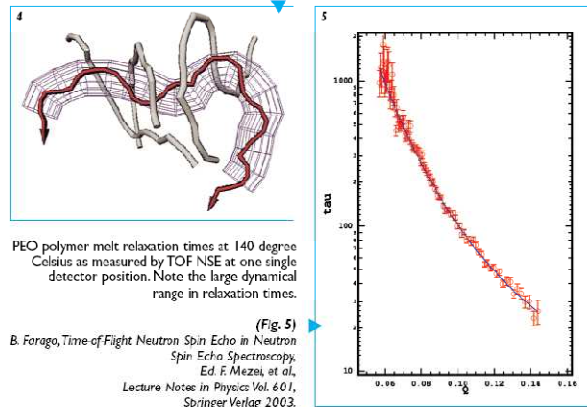


(Fig. 3) Au(0.86)/Fe(0.14) spin glass dynamics. C. Pappas, F. Mezei, G. Ehlers, P. Manuel, I.A. Campbell - *Physical Review B* **68**, 054431 (2003).

(Fig. 4) Polymer reptation for different molecular weight PE polymers. A. Wischniewski, M. Monkenbusch, L. Willner, et al. *Phys. Rev. Lett.* **88** C58301 (2002).



PEO polymer melt relaxation times at 140 degree Celsius as measured by TOF NSE at one single detector position. Note the large dynamical range in relaxation times.

(Fig. 5) B. Forago, *Time of Flight Neutron Spin Echo in Neutron Spin Echo Spectroscopy*, Ed. F. Mezei, et al., *Lecture Notes in Physics* Vol. 661, Springer Verlag 2003.

Instrument description

The spin-echo spectrometer IN15 offers three modes of operation.
 • standard: conventional spin echo using a velocity selector and a neutron guide between selector and precession magnet.
 • focusing option: conventional spin echo using a focusing mirror (developed by FZ Jülich) between selector and precession magnet;
 • tof-option: time-of-flight spin-echo using a triple chopper and a frame overlap filter chopper arrangement. A wide wavelength band is used covering a large area in q-time space even for one single detector position.

Normal mode of operation
 Due to the use of neutrons of long wavelength ($8\text{Å} < \lambda < 25\text{Å}$ in standard mode and $17.5\text{Å} < \lambda < 25\text{Å}$ in focusing mode) IN15 offers a better energy resolution (proportional to λ^2) than IN11 and it reaches considerably lower q-values (proportional to λ^3).

The use of long wavelength neutrons also eases important design problems, e.g.

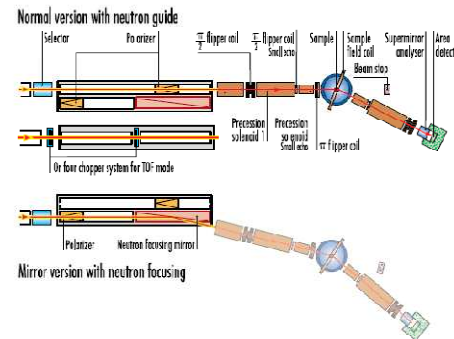
- the neutron polarisation and polarisation analysis;
- the production of smaller precession fields;
- the beam deflection achievable by a single super-mirror ($> 4^\circ$).

The energy resolution is improved by the reduction of possible inhomogeneities of the field integral along different neutron trajectories:
 • special attention has been paid to the manufacturing of the coils;
 • compared to IN11, an increased inner diameter of the solenoidal precession coils of 40 cm has been chosen.

low q-values
 A 2-dimensional position sensitive detector is used to access low q-values. Special care has been paid to reduce parasitic small angle scattering
 • from air;
 • from beam windows;
 • from Fresnel or flipper coils.

further novelties are:
 • a beam splitter, which consists of a 2 m long assembly of TiNi supermirrors deposited on a Si-substrate. It divides the HSI beam into two parts. IN15 uses the reflected beam H511 (cut-off at 4 Å and maximum of the wavelength distribution at 8.6 Å);
 • a magnetic neutron guide with a FeCo layer superimposed on an antireflecting GdTi layer prepoliarises the beam (provided by HMI Berlin). It also offers the advantage to shorten the polariser;
 • flipper coils made of bare aluminium wire which is wound with a calibrated space of 0.5 mm between each turn, the thickness of the coil can be adjusted (between 0.3 and 1 cm) for a better flipping efficiency at any wavelength;
 • large Fresnel coils have been developed to take advantage of nearly the full size of the 2D detector.
 Without $m/2$ flippers simple polarisation analysis experiments can be performed.

Instrument layout



time-of-flight option
 A set of three choppers (variable pulse width: from 1 to 25 ms; pulse repetition rates between 5 and 20 Hz; maximum chopper speed: 9600 rpm) replaces the velocity selector in the primary part of IN15. The operation in time-of-flight together with spin echo provides a large dynamic range.

focusing option
 The incident polarised beam is totally reflected by a toroidal mirror (4 m long) which focusses the beam onto the detector. An intensity gain of a factor 10 is expected at a q-resolution of $3 \times 10^3 \text{Å}^{-1}$ and a factor 100 at 10^3Å^{-1} . The possibility to reach q-values as small as 10^2Å^{-1} will finally provide an overlap to optical spectroscopy.

summary of the performance at $\lambda = 25 \text{Å}$
 • The intensity is sufficiently high for typical small-angle scattering experiments;
 • the energy resolution (1 neV, smallest measurable inelasticity 0.1 neV) is a factor 20 higher than on IN11;
 • the Q-range from 10^2Å^{-1} up to 0.4Å^{-1} ;
 • the time-of-flight operation mode offers a large dynamic range in energy, i.e. four orders of magnitude (0.2 - 2000 neV).

Instrument Data

Location
 Guide hall n°2, cold polarising guide H511

neutron beam characteristics	
diameter at sample position	40 mm (normal operation) 100 mm (focusing option)
incident wavelength	8 to 25 Å
monochromatisation $\Delta\lambda/\lambda$ (PWHM)	15% (velocity selector) 5-50 % (tof option)
incident beam divergence	$< 17 \text{ mrad}$
polariser	V cavity, 1 m long (provided by HMI Berlin)
analyser	FeCo-Si supermirrors on Si substrate (provided by HMI Berlin)

precession coils	
max. field of solenoid	1.5 kG
max. field integral	$2.7 \times 10^3 \text{ Gcm}$

detector	
32 x 32 pixels, each 1 cm ² at a distance of 4.6 m from the sample 1 bar ⁴ He and 0.3 bar CF ₄	
area	32 x 32 cm ²
pixel size	1 cm ²
angular range 2θ	2° to 140°
angular resolution	$2 \times 10^{-3} \text{ rad}$

web: www.ill.fr/YellowBook/IN15/

High-resolution spectrometers

INSTRUMENT

BEAMLINE
15

SPALLATION NEUTRON SOURCE

NSE - NEUTRON SPIN ECHO SPECTROMETER



NSE is the best spectrometer of its class in both resolution and dynamical range. Exploiting superconducting technology and developing novel field correction elements, the maximum achievable Fourier time will be extended to at least 1 μ s. Using wavelengths of $0.25 < \lambda/\text{nm} < 2.0$, an unprecedented dynamical range of six decades from 1 ps $< \tau < 1 \mu$ s can be achieved. The design of the spectrometer takes advantage of recent progress in neutron optics and polarizing supermirror microbenders, resulting in considerable gains in polarized neutron flux over a wide wavelength range. Performance is also extended by a position-sensitive, two-dimensional detector with a broad detection region. As a result, the effective data rate will gain an additional factor of 5 in addition to

the estimated time-averaged sample flux of 10^7 n/cm²s around $\lambda = 1$ nm. This yields the highest available data accumulation rate. In addition, the wavelength distribution width at any time is well below 0.5%, causing the resolution in momentum transfer to increase significantly compared with reactor instruments with 10% or more wavelength distribution width.



APPLICATIONS

Although the NSE spectrometer is designed primarily for soft-matter research, its capabilities also make it useful for all fields of modern condensed matter and materials science. This instrument is especially suited for analyzing slow dynamical processes and thereby unraveling molecular motions and mobilities at nanoscopic and mesoscopic levels. This feature is highly relevant to soft-matter problems in research on the molecular rheology of polymer melts, related phenomena in networks and rubbers, interface fluctuations in complex fluids and polyelectrolytes, and transport in polymeric electrolytes and gel systems. NSE could also aid studies in biophysics and magnetism.

SPECIFICATIONS

Moderator	Cold-coupled hydrogen
Neutron guide $h \times b$	⁹³ Ni coated, 4×8 cm ² , $m = 1.2$
Wavelength selection	Chopper system consisting of four choppers and selecting a wave length band up to 3.66 Å
Accessible wavelength range	$2 \text{ Å} < \lambda < 20 \text{ Å}$
Declination angle	3.5°
Maximum scattering angle	$\pm 80^\circ$
Q range	$0.0025\text{--}0.6 \text{ Å}^{-1}$
Maximum field integral	$J = 1.8 \text{ Tm}$
Dynamic range	$1 \text{ ps} < \tau < 1 \mu\text{s}$
Typical sample size	$30 \times 30 \text{ mm}$
Analyzer	$m=3$ rotatable supermirror
Detector	³ He counter ($300 \times 300 \text{ mm}^2$)
Typical scanning time with 10% scatterer	5 hours/spectrum

Status:
To be commissioned in 2009

FOR MORE INFORMATION, CONTACT

Instrument Scientist: Michael Ohl, ohlme@ornl.gov, 865.574.8426

http://neutrons.ornl.gov/instrument_systems/nse.shtml



August 2007

ORNL-6838 Rev. 1/07

Summary

QENS theory and experiment hand in hand

1959-61 Four early years at Saclay plus subsequent post doc led de Gennes to write his first papers on neutron scattering - from liquids

1965- 75 Spectrometers for quasi-elastic scattering were developed at a number of neutron sources worldwide – especially ILL

1965-75 Physicists and chemists recognised polymers were interesting examples for the neutron techniques. Initially density of states. Quasi-elastic scattering showed much slower q-dependence of the energy broadening than for simple liquids.

1967 Two de Gennes papers in the now defunct *Physics* develop the theory for this unusual q-dependence and indicate the time dependence

1970-80 Scientists search for these t and q-dependences using new high resolution QENS but the convolution problem is a “killer”.

1975-80 Neutron spin-echo spectrometer IN11 is built at ILL – it has higher resolution and also solves the convolution problem.

1981 de Gennes publishes the functional form of the correlation function for one reptating chain

1980-85 First observations using NSE of the effect of entanglements on slowing down the motion of a single polymer molecule. Direct comparisons to the model correlation function

1985 onwards NSE spectrometers are built with increasing count rates and higher resolution. Polymer motion for different chemical and physical structures is observed in increasing detail and compared to more sophisticated models. Molecular dynamics calculations “come of age” and provide a further source of insight.

